Molecular Genetics and Metabolism Reports 13 (2017) 55–63

Contents lists available at ScienceDirect

Molecular Genetics and Metabolism Reports

journal homepage: www.elsevier.com/locate/ymgmr

Case Report

ALG9-CDG: New clinical case and review of the literature

Kellie Davis[a,*,1], Duncan Webster[b], Chris Smith[a], Sheryl Jackson[a], David Sinasac[a], Lorne Seargeant[c], Xing-Chang Wei[d], Patrick Ferreira[a], Julian Midgley[e], Yolanda Foster[f], Xueli Li[f], Miao He[f], Walla Al-Hertani[a]

[a] Department of Medical Genetics, Cummings School of Medicine, University of Calgary, Alberta Children's Hospital, Calgary, Alberta, Canada
[b] Department of Medicine, Dalhousie University, Saint John, New Brunswick, Canada
[c] Department of Clinical Biochemistry and Genetics, Diagnostic Services Manitoba, Department of Pediatrics, University of Manitoba, Winnipeg, Manitoba, Canada
[d] Department of Diagnostic Radiology, University of Calgary, Alberta Children's Hospital, Calgary, Alberta, Canada
[e] Department of Pediatrics, University of Calgary, Alberta Children's Hospital, Calgary, Alberta, Canada
[f] Department of Medical Genetics, Children's Hospital of Philadelphia, Philadelphia, PA, United States

ARTICLE INFO

Keywords:
Congenital disorders of glycosylation
ALG9-CDG
CDG-IL
ALG9
Transferrin isoelectrofocusing type 1 pattern
Lethal skeletal dysplasia

ABSTRACT

Congenital disorders of glycosylation (CDG) are a group of metabolic diseases resulting from defects in glycan synthesis or processing. The number of subgroups and their phenotypic spectrums continue to expand with most related to deficiencies of N-glycosylation. ALG9-CDG (previously CDG-IL) is the result of a mutation in *ALG9*. This gene encodes the enzyme alpha-1,2-mannosyltransferase. To date, a total of 10 patients from 6 different families have been reported with one of four *ALG9* mutations. Seven of these patients had a similar phenotype with failure to thrive, dysmorphic features, seizures, hepatic and/or renal cysts; the other three patients died *in utero* from a lethal skeletal dysplasia. This report describes an additional patient with ALG9-CDG who has a milder phenotype. This patient is a term female born to Caucasian, Canadian, non-consanguineous parents of Scottish decent. Prenatally, dysmorphic features, numerous renal cysts and minor cardiac malformations were detected. Post-natally, dysmorphic features included shallow orbits, micrognathia, hypoplastic nipples, talipes equinovarus, lipodystrophy and cutis marmorata. She developed failure to thrive and seizures. The metabolic work-up included analysis of a transferrin isoelectric focusing, which showed a type 1 pattern. This was confirmed by glycan profiling, which identified ahomozygous mutation in *ALG9*, c.860A > G (p.Tyr287Cys) (NM_1234567890). This had been previously published as a pathogenic mutation in two Canadian patients. Our goal is to contribute to the growing body of knowledge for this disorder by describing the phenotypic spectrum and providing further insight on prognosis.

1. Introduction

Congenital disorders of glycosylation (CDG) are a rare group of metabolic diseases that can affect multiple organ systems. They are caused by defects in glycoprotein and glycolipid glycan synthesis, attachment and modification. These complex processes require numerous enzymes for transportation of lipid-linked oligosaccharides across the endoplasmic reticulum (ER) membrane, sequential addition of sugar groups and further processing within the golgi apartus; the majority of these disorders are related to N-glycosylation [3]. Currently, the most widely used test to screen for N-glycosylation defects assesses transferrin isoforms by transferrin isoelectric focusing (TIEF); patients identified to have an abnormal pattern can be further assessed by glycan profiling [3,6].

ALG9-CDG (previously CDG-IL) was first described by Frank et al. [4] in a term female born as a twin in Europe in whom they found a homozygous point mutation, NM_024740.2: c.(1588G > A), p.(Glu530Lys), rs 121908022. Two additional patients with ALG9-CDG were published in 2005 and 2009, by Weinstein and Vleugels, respectively. Both patients were found to be homozygous for NM_024740.2: c.(860A > G), p.(Tyr287Cys), rs 121908023. In 2015, Tham et al. [10] reported three additional patients with *ALG9* mutations in fetuses with lethal skeletal dysplasias further expanding on the known phenotype. The two females and one male were from different consanguineous Middle Eastern families and were homozygous for NG_009210.1: g.(35929T > A), NM_024740.2: c.(1173 + 2T > A); the authors suggested the possibility of a founder mutation as one potential explanation. In 2015, another four related patients with ALG9-CDG were

* Corresponding author at: Department of Medical Genetics, Alberta Children's Hospital, 2888 Shaganappi Trail NW, Calgary, Alberta T3B 6A8, Canada.
E-mail address: kellie.davis@saskatoonhealthregion.ca (K. Davis).
[1] Present address: Room 515, Ellis Hall, Royal University Hospital, 103 Hospital Drive, Saskatoon, SK, S7N 0W8.

http://dx.doi.org/10.1016/j.ymgmr.2017.08.004
Received 15 May 2017; Received in revised form 19 August 2017; Accepted 20 August 2017
Available online 06 September 2017

reported by AlSubhi et al. [1]. The patients were part of a large, consanguineous Saudi Arabian family and were homozygous for the mutation also reported by Frank et al. [4], c.(1588G > A), p.(E530K).

With increased availability and decreased cost of multi-gene molecular based panels and whole exome sequencing, patients are being diagnosed with CDG's, more frequently. Previously, this category of disorders fell lower on the differential or had not been considered at all, as with patients who had few or isolated systems affected such as the heart or skeleton.

The goal of this report is to contribute to the growing body of knowledge regarding the ALG9-CDG subtype by comparing the known patients, providing clinical updates on those patients previously reported, and describing the mutations in relation to their position relative to the protein domains.

2. Patient report

The patient was born to a healthy 23-year-old G4 P0 woman. The parents were Caucasian and non-consanguineous. At the first trimester screen, a slightly increased nuchal translucency measured 2.8 mm while the screen itself was negative. At the 19-week anatomy scan, the right kidney was noted to be largely replaced by numerous cysts and the left kidney slightly hyperechogenic (Fig. 1). Dysmorphic features were visualized including a short neck, micrognathia, a long philtrum, and prefrontal edema (Fig. 1). A fetal echocardiogram showed mild prominence of the right ventricular free wall with normal function. Growth was appropriate for dates throughout gestation. An amniocentesis was performed with a normal female 46,XX result.

Delivery occurred at 37 weeks and 5 days' gestation *via* vaginal delivery. The birth weight was 3255 g (25-50th percentile), length 48 cm (25th percentile), and head circumference 34 cm (50–90th percentile). The patient developed respiratory distress, was intubated and transported to the NICU where she was placed on nitric oxide. An echocardiogram showed severely reduced biventricular function and pulmonary hypertension requiring support with prostaglandins and milrinone, which resolved after three days.

Physical examination showed slightly splayed sutures, upslanting palpebral fissures, a triangular nose, long philtrum and micrognathia (Fig. 2). Irregular fat distribution was noted around the buttocks and lower back. Nipples were hypoplastic and widely spaced (Fig. 2). Wrists were held in flexion with adducted thumbs, knees and ankles contracted and the toes were broad. There was extensive cutis marmorata.

Serial repeat echocardiograms showed a small atrioseptal defect (ASD), slightly small aortic isthmus and a functionally bicuspid aortic valve. On abdominal ultrasound and a lasix renal scan (a nuclear medicine study which assesses renal function by measuring the content of dye filtered from the blood into the collecting ducts), the right kidney was described as almost completely replaced with cysts and non-functional; the left kidney had small, scattered cysts but functioned normally (Fig. 1). The baseline serum creatinine remained within the low-normal range. Small cysts were seen in the liver, which did not appear to impact liver function based on chemistry results (Fig. 1).

At five months of age she had her first seizure. A neurological workup included a magnetic resonance imaging (MRI) of the brain, which showed normal structure, mildly delayed myelination, and non-enhancing areas of diffusion restriction in superior cerebellar peduncles, medial cerebral peduncles, midbrain and hypothalamus (Fig. 3). A follow-up brain MRI at the age of 25 months showed no focal lesion in the brain. The myelination was appropriate for age, but a diffuse mild to moderate cerebral atrophy had developed; no cerebellar atrophy was detected (Fig. 3).

Poor weight gain and feeding issues were ongoing concerns with growth parameters falling to - 2-to-3 standard deviations. By 14 months of age, she had been admitted to hospital 6 times for failure to thrive or seizure management. Developmental delay had been seen in all domains and she was unable to sit unassisted or make discrete sounds. A skeletal survey targeted towards identifying the specific changes described in the report by Tham et al. [10] was normal.

At the age of two-and- a-half years she continued to have seizures and developmental.

delay with difficulty gaining weight, but was otherwise relatively well, requiring less frequent hospitalization and slowly making developmental progress. Unfortunately, however, the patient passed away while admitted to hospital with pneumonia and renal failure at 2 years

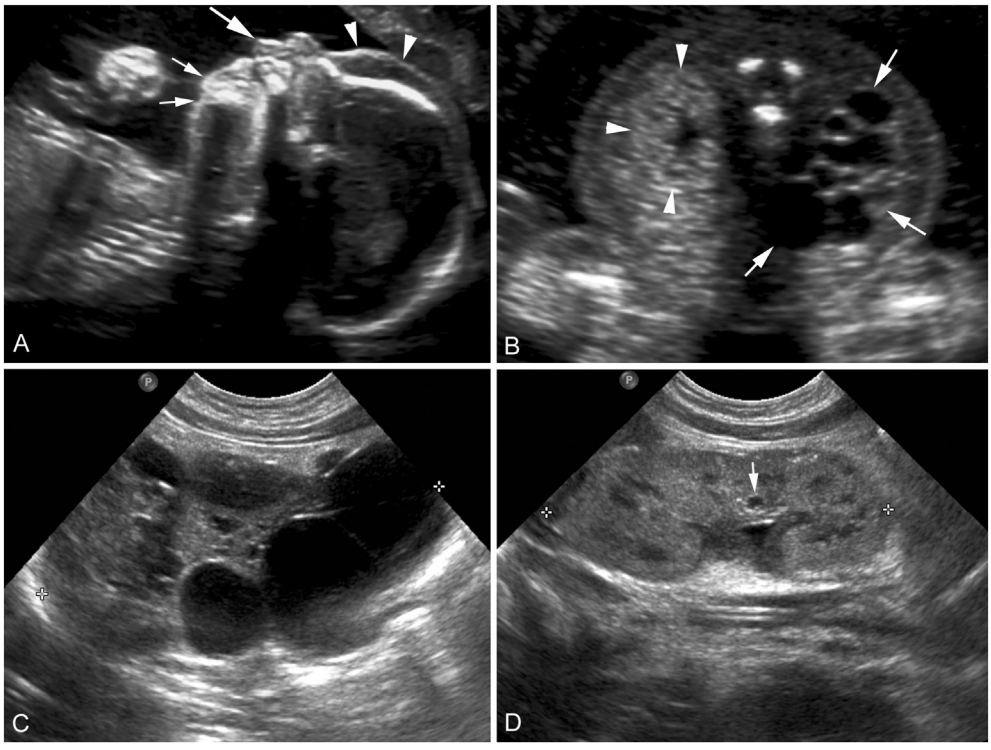

Fig. 1. Obstetrical ultrasound images from the 19 weeks' gestation anatomy scan (A, B) and post-natal renal ultrasound images obtained at day two of life (C, D). Sagittal facial profile view (A) shows prefrontal edema (arrowheads), a long philtrum (large arrow), and micrognathia (small arrows). An axial view through fetal kidneys (B) shows a markedly enlarged right kidney (arrows) in which the renal parenchyma is nearly completely replaced with simple cysts of variable sizes. The axial view also shows a morphologically normal but slightly echogenic left kidney (arrowheads). Post-natal sagittal ultrasound image of the right kidney (C) again shows a multicystic dysplastic kidney (cursors). Post-natal sagittal ultrasound image of the left kidney (D) shows morphologically normal left kidney (cursors) with a small simple cyst (arrow).

Fig. 2. (left to right, top to bottom) Clinical photographs of the patient at 3, 6, and 14 months of age. Dysmorphic features shown here include hypertelorism, shallow orbits, smooth philtrum, micrognathia, fleshy ears, hypoplastic nipples and cutis marmorata. [Color figure can be viewed in the online issue, which is available at http://onlinelibrary.wiley.com/journal/10.1002/(ISSN)1552-4833.]

and 10 months of age.

3. Material and methods

3.1. Cytogenetic investigations

A G-banded karyotype was performed on cultured amniocytes obtained by amniocentesis at 20 weeks and 1 day of gestation. Post-natally, comparative genomic hybridization (CGH) oligoarray using the platform CytoChipTM ISCA 8x60K v2.0 was performed on DNA extracted from peripheral whole blood.

3.2. Transferrin isoelectric focusing

Serum samples were qualitatively analyzed by isoelectric focusing and subsequent transferrin immunofixation as described by Stibler et al. in 1979 [9].

3.3. Glycan analysis

An N-glycan profile of fibroblast total cellular protein was obtained as previously described [2] with minor modification. Fibroblasts were cultured in a modification of Eagle medium containing 1000 mg/L D-glucose (Corning Cellgro, Manassas, Virginia, USA), with 10% fetal bovine serum (Invitrogen, Carlsbad, California, USA) and antibiotics-antimycotics (Invitrogen), until 100% confluence in a T75 culture flask. The cells were then washed twice with PBS and harvested using a cell scraper. Fibroblast pellets were washed 3 times with PBS by centrifugation and then lysed in 200 µL PBS. Subsequently, 200 µg cellular protein from the cell lysate was denatured and precipitated with 2 × volume of 100% propanol. N-linked glycans were released from precipitated protein, using the PNGase F kit from New England Biolabs (Ipswich, Massachusetts, USA). The released N-linked glycans from total cell lysate were purified and desalted by solid phase extraction using a SepPak C18 and carbograph column. N-linked glycans were permethylated with sodium hydroxide and iodomethane in dimethyl sulfoxide (DMSO). After permethylation, glycans were extracted with water/chloroform (2:1, vol/vol) in four steps and dried samples were then dissolved in 50% methanol, spotted with 11% 2,5-dihydroxylbenzoic acid matrix (1:1 vol/vol), and measured by matrix-assisted laser desorption and ionization time-of- flight mass spectrometry (MALDI-TOF MS) using the positive mode on Ultraflex MALDI-TOF/TOF system (Bruker Daltonics, Massachusetts, USA). N-glycans in plasma were released from total plasma protein, purified and permethylated as described by Xia [13] and analyzed by an Ultraflex MALDI-TOF/TOF system as described above.

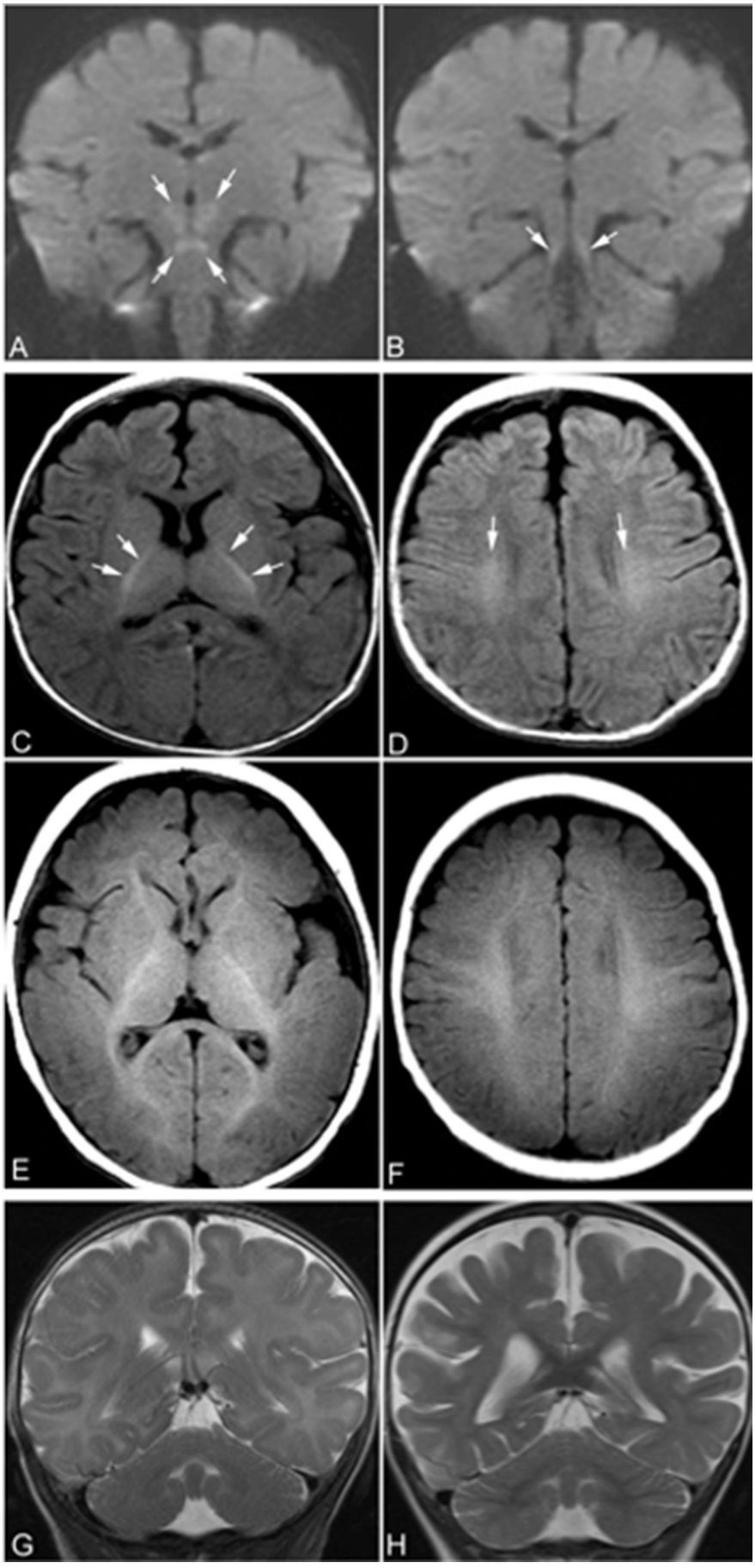

Fig. 3. Brain MRI. At 4 months of age, an MRI of the brain shows restricted diffusion symmetrically in the superior cerebellar peduncles, midbrain, and hypothalamus (arrows in A and B). On axial T1-weighted images obtained at 4 months of age (C and D), myelination of white matter was only seen in the posterior limbs of internal capsule (arrows in C) and small areas of corona radiata (arrows in D). The myelinated white matter is hyperintense relative to the unmyelinated white matter. At 4 months of age, myelination of white matter should be seen in anterior limbs of internal capsule, optic radiations, splenium of corpus callosum, and subcortical white matter in peri-rolandic regions, as shown in the T1-weighted MR images of a normal subject obtained at the same age (E and F). The delayed myelination of the patient is easily appreciated by compared the patient's T1-weighted images to those images of the normal subject. The coronal T2-weighed images of the patient obtained at 4 months of age (G) does not show cerebral or cerebellar atrophy. However, coronal T2-weighted images at the same level obtained at 25 months of age (H) shows signs of mild to moderate global cerebral atrophy including dilatation of lateral ventricles, prominent subarachnoid spaces, and including widened cerebral sulci. No cerebellar atrophy was present on either of the MRI scans.

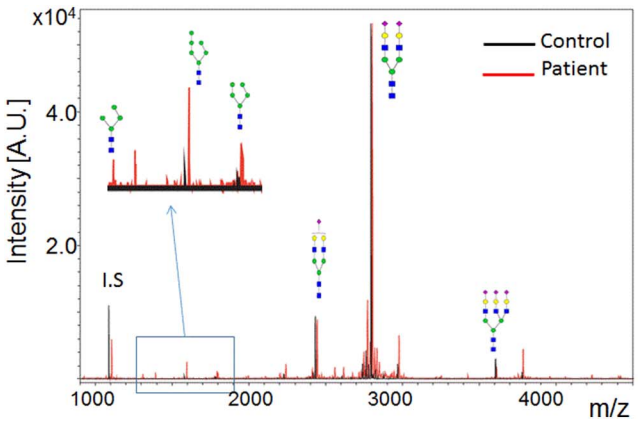

Name	% Total	Reference range	
Man4GlcNAc2	0.30%	0.00%	H
Man5GlcNAc2	1.25%	0-0.99%	H
Man6GlcNAc2	0.48%	0-0.35%	H
Man7GlcNAc2	0.00%	0-0.08%	
Man8GlcNAc2	0.00%	0-0.23%	
Man9GlcNAc2	0.00%	0-1.01%	

Fig. 4. N-glycan profile in plasma for a normal control (left) and this patient (right) showing elevations in species with 4, 5, and 6 mannose units, consistent with dysfunction of alpha-1,2-mannosyltransferase. [Color figure can be viewed in the online issue, which is available at http://onlinelibrary.wiley.com/journal/10.1002/(ISSN)1552-4833.]

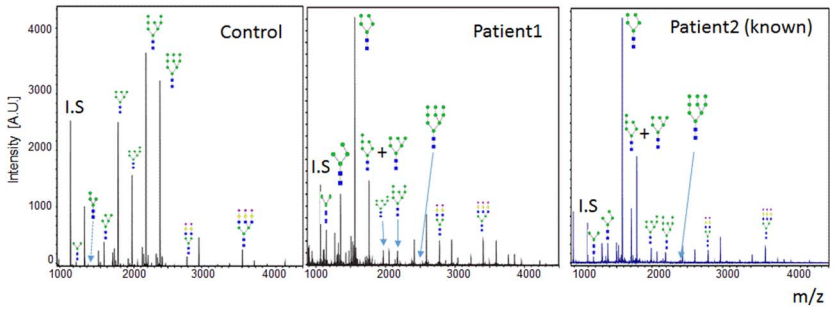

Fibroblast N-glycans

Name	P2	P1	Reference range	
Man4GlcNAc2	2.95%	6.11%	0-1.84%	H
Man5GlcNAc2	41.82%	29.30%	1.8-14.3%	H
Man6GlcNAc2	19.28%	12.03%	7.5-15.8%	H
Man7GlcNAc2	2.72%	1.95%	4.9-12.7%	L
Man8GlcNAc2	2.26%	1.87%	9.8-32.9%	L
Man9GlcNAc2	0.29%	0.42%	7.2-32%	L

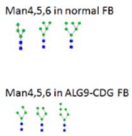

Fig. 5. N-glycan profile in fibroblasts for a normal control (left), this patient (center) and a second patient with ALG9-CDG reported by Vleugels et al. [11] (right) showing elevations in species with 4, 5, and 6 mannose units, consistent with dysfunction of alpha-1,2-mannosyltransferase. [Color figure can be viewed in the online issue, which is available at http://onlinelibrary.wiley.com/journal/10.1002/(ISSN)1552-4833.]

3.4. Sanger sequencing of ALG9 in gDNA and cDNA

Genomic DNA (gDNA) extracted from blood and complimentary DNA (cDNA) synthesized from mRNA extracted from cultured skin fibroblast of the patient were used for polymerase chain reaction (PCR) amplification of cDNA that covered the whole coding sequence as well as exons of *ALG9* in gDNA following standard protocols described above.

4. Results

4.1. Biochemical testing

The patient's newborn metabolic screen was normal (disorders screened for as posted on www.health.alberta.ca in 2014). Plasma amino acids, urine organic acids, plasma acylcarnitine profile and very-long chain fatty acids were all normal. Serum biotinidase, serum 7-dehydrocholesterol, urinary 3-methylglutaconic acid, sialic acid, uronic acid and oligosaccharide electrophoresis were also normal.

4.2. Cytogenetic investigations

The karyotype was a normal female karyotype, 46,XX. The array CGH was normal.

4.3. Transferrin isoelectric focusing

Serum for this patient was tested for evidence of a CDG by evaluation of immunoreactive forms of serum transferrin after isoelectric focusing in polyacrylamide gels. The serum transferrin focusing pattern showed decreased tetrasialo-Tf along with increased disialo-Tf and small amounts of asialo-Tf (type 1). The sample was consistent with CDG type I. The sample was sent to Mayo Medical Laboratories (Rochester, Minnesota, United States), which confirmed this finding by liquid chromatography mass spectrometry (LC-MS).

4.4. Glycan profiling

N-glycan profile of our patient showed significant increase of N-linked GlcNAc2Man4, GlcNAc2-Man5 and GlcNAc2-Man6 with absence of N-linked GlcNAc2Man7, N-linked GlcNAc2Man8 and GlcNAc2Man9 (Fig. 4). The blockage of N-glycan biosynthesis after Man6 indicated a probable defect in *ALG9*. In order to confirm the N-glycan changes seen in the plasma total glycoproteins, we next examined N-glycan profiles from total cellular protein of cultured skin fibroblast from the patient. N-linked high mannose species on fibroblast cellular proteins are much more abundant than those on secreted plasma glycoproteins since N-linked high mannose glycans from the ER- or Golgi-associated trimming processes are present intracellularly. Consistent with the plasma N-glycan profile, significant reduction of N-linked Man7, Man 8 and Man9 were observed in the patient's fibroblasts with increased N-Man6, Man5 and Man4 (Fig. 5). This pattern was consistent with a blockage of N-glycan biosynthesis at the step encoded by *ALG9*. Interestingly, the most dramatic increase of truncated N-glycan appears to be N-linked Man5, which suggests further trimming of N-linked Man6 by ER and Golgi associated glycan trimming. We predict that N-Man4, 5, 6 present in ALG9-CDG fibroblast have glycan profiles different from those in normal fibroblast (Fig. 5).

4.5. Molecular sequencing

Sequencing of *ALG6*, *MPI*, *PMM2* (first tier) and *ALG12*, *ALG2*, *ALG3*, *ALG8*, *DPM1*, *MPDU1* (second tier) were all normal (Prevention Genetics, Wisconsin, United States). Based on the glycan profile, sequencing of *ALG9* was performed. A homozygous mutation, c.(860A > G), p.(Y287C), was detected. Parental studies were carried out and both parents were found to carry one copy of c.(860A > G) mutation.

Table 1
Characteristics of the 11 known patients with ALG9-CDG.

Feature	Frank et al. [4]	Weinstein et al. [12]	Vleugels et al. [11]	Tham et al. [10], Patient 1	Tham et al. [10], Patient 2	Tham et al. [10], Patient 3	AlSubhi et al. [1], Patient 1	AlSubhi et al. [1], Patient 2	AlSubhi et al. [1], Patient 3	AlSubhi et al. [1], Patient 4	Davis et al. [2]
Sex	Female	Female	Female	Female	Male	Female	Female	Male	Female	Male	Female
Ethnicity	Not included	Canadian, Caucasian	Canadian, Caucasian	Turkish	Iraqi	Iraqi	Saudi Arabian	Saudi Arabian	Saudi Arabian	Saudi Arabian	Canadian, Caucasian
Consanguinity	No	No	No	Yes	Yes	Yes	Yes	Yes	Yes	Yes	No
Homozygous ALG9 mutation (NM_024740.2)	c.1567G > A, p.E523K	c.860A > G, p.Y287C, rs 121908023	c.860A > G, p.Y287C, rs 121908023	c.1173 + 2T > A; p.V340Afs*57	c.1173 + 2T > A; p.V340Afs*57	c.1173 + 2T > A; p.V340Afs*57	c.1588G > A; pE530K	c.1588G > A; pE530K	c.1588G > A; pE530K	c.1588G > A; pE530K	c.860A > G; p.Y287C
Prenatal history	Not included	Pericardial effusion	Not included	Oligohydromnios, enlarged and hyperechogenic kidneys, large ventriuloseptal defect, anomalous outflow tract	Brachymelia, low-set ears, micrognathia, enlarged and hyperechogenic kidneys, hydronephrosis, hydrops		Decreased fetal movements	Not included	Not included	Hydrops fetalis	Prefrontal edema, micrognathia, short neck, long philtrum, polycystic kidneys
Growth parameters	Severe microcephaly	Weight < 3rd, length < 3rd, head circumference 3rd; progressive microcephaly	Not included	Birth weight 0.8 SD, length −2SD, head circumference −2 SD.	Birth weight −1.5 SD, length −1.6 SD, head circumference −1.3 SD	Not included	All growth parameters at the 5th percentile by age 6 years	Microcephaly	Microcephaly	Birth weight > 97th percentile; no microcephaly	Birth weight 25–50th, birth length 25th, head circumference 50–90th; at 3 months weight −3 SD, length −2 SD, OFC −2 SD
Dysmorphisms	Not included	Inverted nipples	"Mild"	Brachycephaly, wide anterior fontanelle, frontotemporal hypertrichosis, proptosis, hypertelorism, telecanthus, beaked nose, hypoplastic nasal alae, flat philtrum, thin upper lip, retromicrognathia, low-set posteriorly rotated fleshy ears, excess nuchal skin			Scalp cutis aplasia, bossing, hypertelorism, depressed nasal bridge, large mouth, low-set ears, widely spaced inverted nipples, lipodystrophy	"Yes"	"Yes"	Skin edema at birth, short nose, long philtrum, short neck	Splayed sutures, metopic ridge, shallow orbits, discordant gaze, low columnella, smooth philtrum, thin upper lip, bifid uvula, micrognathia, rotated ears, short wide neck excess nuchal skin, low posterior hairline, hypoplastic nipples, cutis marmota
Seizures	Present	Present	Present	N/A	N/A	N/A	Present	Present	Present	Present	Present
Central nervous System	Hypotonia	Hypotonia, irritability, intermittent esotropia, head lag, increased cerebrospinal fluid spaces, widened sulci, delayed myelination, cerebral/ cerebellar atrophy	Mild hypotonia, inconsolable crying	Not included	Not included	Not included	Hypotonia, exaggerated deep tendon reflexes; cerebral and cerebellar atrophy; delayed myelination			Hypotonia, wide subarachnoid spaces	Hypotonia, irritability, spacticity in the legs, mildly delayed myelination, diffusion restriction in superior cerebellar peduncles/medial cerebral peduncles/ midbrain/ hypothalamus
Cardiorespiratory	Bronchial asthma	Pericardial effusion, this lead	Small pericardial	"Congenital heart defect", lung	Lung hypoplasia, abnormal lobation		Mild tricuspid regurgitation	Not included	Mild pericardial	Atrioseptal defect, mild	Atrioseptal defect, ventriculoseptal

(continued on next page)

Table 1 *(continued)*

Feature	Frank et al. [4]	Weinstein et al. [12]	Vleugels et al. [11]	Tham et al. [10], Patient 1	Tham et al. [10], Patient 2	Tham et al. [10], Patient 3	AlSubhi et al. [1], Patient 1	AlSubhi et al. [1], Patient 2	AlSubhi et al. [1], Patient 3	AlSubhi et al. [1], Patient 4	Davis et al. [2]
		to tamponade	effusion	hypoplasia, abnormal lobation					effusion	dilatation of the right ventricle	defect
Genitourinary	Not included	Not included	Not included	Polycystic kidneys, hypoplastic renal arteries/ureters/ bladder, bicornuate uterus, atrophic ovaries	Polycystic kidneys	Polycystic kidneys, hydronephrosis, bicornuate uterus	Not included	Not included	Not included	Not included	Polycystic, dysplastic kidneys
Gastrointestinal	Hepatomegaly	Focal villous atrophy in the small bowel	Vomiting, watery stool	Periportal fibrosis	Not included	Omphalocele	Mild hepatomegaly	Mild hepatomegaly	Mild hepatomegaly	Mild hepatomegaly	Multiple small liver cysts, gastroesophageal reflux
Musculoskeletal	Not included	Right-sided torticollis, severely decreased muscle bulk	Not included	Decreased ossification of the frontoparietal bones, thickened occiput, absent ossification of cervical spine, brachymelia, ulnar deviation of the hands, decreased ossification of the pubic bones, round pelvis, shortened greater siatic notches, ovoid ischia, short tubular bones with metaphyseal flaring			Mild skeletal dysplasia				Talipes equinovarus, adduction of thumbs

5. Discussion

In 2004, the first patient with ALG9-CDG was reported with additional case reports published in 2005 and 2009; in 2015 alone, another seven patients were described. To the best of our knowledge, there are only eleven patients reported in the literature (including this patient), however, some trends appear to be emerging with most patients being moderately affected and only a few with a lethal skeletal dysplasia (for full details, please see Table 1).

For the less severe group, cystic kidneys and hydrops fetalis seem to be among the most striking clinical findings. While both are non-specific, they have relatively shorter differentials than the dysmorphic features (Table 1). In contrast, the reports which involved intrauterine demise had similar dysmorphic features but with significant skeletal abnormalities. Perhaps the constellation of findings, moderate or severe, could suggest the diagnosis at the time of detection, facilitating rapid carrier testing in parents ultimately allowing for timely prenatal diagnosis and planning. Post-natally, common findings include: frontal bossing, hypertelorism, depressed nasal bridge, large mouth, low-set ears, widely spaced and inverted nipples, and an abnormal distribution of fat. For this patient, possibly less common features include cutis marmorata, equinovarus talipes, flexion of the wrists, and contractures in the knees and ankles.

Delayed myelination is a consistent finding on neuroimaging of the published patients [1,12]. This was also seen in our patient. Global cerebral and cerebellar atrophy was a consistent finding in all the published patients with brain MRI [1,12]. Like in many genetic and neurometabolic syndromes, cerebral atrophy may not present in early stages of the disease but on follow-up MRI of our patient at 25 months, cerebral atrophy was present. On the earlier MRI of our patient, symmetric areas of restricted diffusion were present in in the superior cerebellar peduncles, midbrain, and hypothalamus, which seem not to have been reported before in patients with CDG. The cause of restricted diffusion in this patient is difficult to ascertain. A common cause of restricted diffusion of brain parenchyma is cytotoxic edema and myelin edema [8]. Given the involvement of the superior cerebellar peduncles, which are white matter bundles expected to be myelinated at birth (Reference: Parazzini C, Bianchini E, and Triulzi F. Myelination. In: Tortori-Donati P, Rossi A, Biancheri R, editors. Pediatric Neuroradiology. Berlin: Springer-Verlag; 2005. p. 21–40.), we postulated that myelin edema is possible. On the other hand, the areas of restricted diffusion in the midbrain and hypothalamus appear to be in the nuclei given their location and shape, cytotoxic edema is also possible. Also of note was the lack of cerebellar involvement in this patient; cerebellar findings are quite common among the various types of CDG.

Information on the clinical course of ALG9-CDG is limited by the young age at which the patients were diagnosed and reported before any long-term follow-up had occurred. Most were hypotonic and developed seizures within the first year of life. The patient described by Weinstein et al. passed away before the age of two years as a result of a respiratory failure secondary to a viral illness, shortly after publication [Weinstein, personal communication, 2014]. No update was available for the patient reported by Frank et al. [4]. The young female reported by Vleugels et al. [11] is alive at age 10 years. She has significant physical and cognitive developmental delay. She is generally non-verbal with frequent seizures requiring anti-convulsant medication. She is ataxic and unable to walk. She has cystic kidneys and at the age of two years developed severe sepsis in the setting of a large peri-nephric abscess secondary to an *Escherichia coli* infection. A second episode of severe sepsis occurred at the age of nine years due to influenza B. She has a predisposition to a prolonged QT interval and a small chronic pericardial effusion, though cardiac function is not impacted. The young female described in this report is now two-and-a-half years of age. She continues to have seizures and developmental delay with difficulty gaining weight, but is otherwise relatively well requiring less frequent hospitalization and slowly making developmental progress.

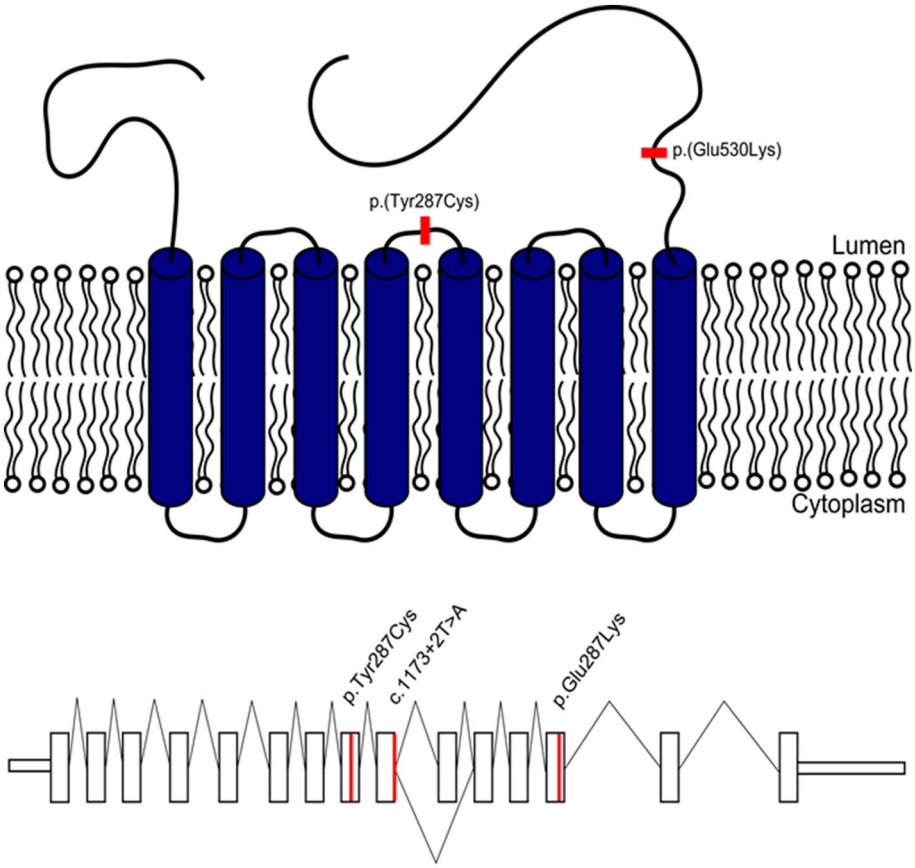

Fig. 6. The top panel displays the locations of the two missense mutations within the predicted protein structure of the *ALG9* protein. Both mutated residues are exposed to the ER lumen rather than residing in the cytoplasmic or predicted transmembrane domains. While the mutations are not located close together in the linear sequence of the protein, they could have close proximity in the protein tertiary structure. The bottom panel displays all three known *ALG9* mutations in a linear schematic. With the limited data available thus far, there does not appear to be clustering to a particular region of the gene. The splicing mutation (c.1173 + 2T > A) causes skipping of exon 10 resulting in an out of frame transcript. [Color figure can be viewed in the online issue, which is available at http://onlinelibrary.wiley.com/journal/10.1002/(ISSN)1552-4833.]

There are three reported *ALG9* mutations: p.(Tyr287Cys) [11,12], p.(Glu530Lys) [1,4] and c.(1173 + 2T > A) [10] (Fig. 6). With such a limited number of mutations presently reported, discussion of genotype-phenotype correlations is speculative at best. Nonetheless, the splicing mutation is associated with the most severe prenatal lethal presentation of the disease and the missense mutations are associated with a less severe disease course. It is impossible to comment on any clustering of the disease-causing mutations with such a small sample size, but both mutations affect residues on the lumenal side of the transmembrane protein (Fig. 6).

The mutation c.(860A > G); p.(Y287C) was not detected in any of the Canadian databases of exomes and whole genome sequences collected and analyzed through various projects including the Care-for-Rare project performed out of the Children's Hospital of Eastern Ontario (CHEO). It was reported on the ExAC database with no homozygotes, 1 allele was found in an East Asian person and 6 in European (non-Finnish) individuals, giving an allele frequency of 5.833e − 05 (http://exac.broadinstitute.org).

While there are too few patients for a thorough analysis, one possible explanation for the homozygous mutations in the unrelated Canadian with Scottish ancestry and Middle Eastern families could be a result of two different founders. This could be further analyzed by haplotype analysis if more patients became available for study.

Regarding the glycan profiling, in the past, all of the ER-associated CDG were grouped as CDG-I, on the basis of a type 1 serum transferrin pattern. We believe that this assignment is misleading; using clinically-validated glycomic analysis by mass spectrometry, we find that glycoproteins such as transferrin and immunoglobulins secreted into the blood stream of most type I CDG patients are not only under-glycosylated, but actually contain abnormal N-linked glycans from incomplete glycosylation [6]. Our finding of plasma and fibroblast abnormal N-glycan profiles in ALG9-CDG patients further challenge the traditional view that deficiencies in type I CDG genes only affect the formation of the lipid-linked oligosaccharides (LLO), the precursors of glycosylation, but not the structure of protein-linked N-glycans. More importantly, our finding of abnormal N-glycans on secreted plasma glycoproteins suggests that aberrantly glycosylated glycoproteins escape the ER-associated quality control (ERQC) system, raising the questions of how they actually escape and what the consequence of escaping may be. These questions certainly warrant future studies with respect to the pathogenesis of ALG9-CDG.

Lastly, Man8 on LLO or newly synthesized N-Man8 was previously reported in ALG9-CDG cells by metabolic labeling using radiolabelled mannose under glucose restricted culture condition [11]. However, we did not observe the increase of N-linked Man8 on cellular proteins from ALG9-CDG fibroblast lines at steady state from two ALG9-CDG patients that we have studied here. This may be related to upregulated *ALG12* expression levels under glucose and mannose restricted culture condition. It is possible that overexpression of *ALG12* in ALG9-CDG may bypass the step of 1,2 mannose addition on branch B and produce a Man8 glycan with intact branch C. This is assuming that the 1,2 mannose addition on branch C is highly efficient, and that residual enzyme activity in the patients is sufficient to complete the step or an alternative mannosyltransferase is able to catalyze 1,2 mannosylatransferring on branch C. Regardless, such Man8 species are likely transient species and are not a major N-glycan at the steady state in *ALG9* cells [5].

Through the increasing use of large multi-gene molecular panels and whole exome sequencing, patients with isolated symptoms or those who would not be identified as having a CDG based on serum isoelectric focusing, are being diagnosed. In addition, the use of exomes has also lead to the discovery of new genes in patients with a CDG.

6. Conclusion

In conclusion, ALG9-CDG remains an extremely rare disorder with

most patients having facial dysmorphisms, CNS involvement, mild cardiac defects and polycystic kidneys, while those patients with seemingly more severe mutations develop a lethal skeletal dysplasia. At least one of the moderately affected patients has survived to mid-childhood. Based on the homozygous mutations in unrelated families, two separate founders (one Scottish, one Middle Eastern) may be a possible explanation. More patients are needed to determine the full breadth of the phenotypic spectrum in this disorder.

Acknowledgments

We would like to thank our patient and her family for their participation and continuous support of this project. We would also like to thank Jacek Majewski and Eric Bareke for reviewing the available Canadian databases.

References

[1] S. AlSubhi, A. AlHashem, A. AlAzami, K. Tlili, S. AlShahwan, D. Lefeber, F.S. Alkuraya, B. Tabarki, Further delineation of the ALG9-CDG phenotype, JIMD Rep. 27 (2015) 107–112.

[2] M. Davids, M. Kane, M. He, L. Wolfe, X. Li, M. Raihan, K. Chao, W. Bone, C. Boerkoel, W. Gahl, C. Toro, Disruption of Golgi morphology and altered protein glycosylation in PLA2G6-associated neurodegeneration, J. Med. Genet. 53 (3) (2016) 180–189.

[3] E.A. Eklund, H.H. Freeze, The congenital disorders of glycosylation: a multifaceted group of syndromes, NeuroRx 3 (2) (2006 Apr) 254–263.

[4] C.G. Frank, C.E. Grubenmann, W. Eyaid, E.G. Berger, M. Aebi, T. Hennet, Identification and functional analysis of a defect in the human *ALG9* gene: definition of congenital disorder of glycosylation type IL, Am. J. Hum. Genet. 75 (2004) 146–150.

[5] Z. Hong, H. Kajiura, W. Su, H. Jin, A. Kimura, K. Fujiyama, J. Li, Evolutionarily conserved glycan signal to degrade aberrant brassinosteroid receptors in Arabidopsis, Proc. Natl. Acad. Sci. U. S. A. 109 (28) (2012) 11437–11442.

[6] A.N. Hoofnagle, J.R. Whiteaker, S.A. Carr, E. Kuhn, T. Liu, S.A. Massoni, S.N. Thomas, R.R. Townsend, L.J. Zimmerman, E. Boja, J. Chen, D.L. Crimmins, S.R. Davies, Y. Gao, T.R. Hiltke, K.A. Ketchum, C.R. Kinsinger, M. Mesri, M.R. Meyer, W.J. Qian, R.M. Schoenherr, M.G. Scott, T. Shi, G.R. Whiteley, J.A. Wrobel, C. Wu, B.L. Ackermann, R. Aebersold, D.R. Barnidge, D.M. Bunk, N. Clarke, J.B. Fishman, R.P. Grant, U. Kusebauch, M.M. Kushnir, M.S. Lowenthal, R.L. Moritz, H. Neubert, S.D. Patterson, A.L. Rockwood, J. Rogers, R.J. Singh, J.E. Van Eyk, S.H. Wong, S. Zhang, D.W. Chan, X. Chen, M.J. Ellis, D.C. Liebler, K.D. Rodland, H. Rodriguez, R.D. Smith, Z. Zhang, H. Zhang, A.G. Paulovich, Recommendations for the generation, quantification, storage, and handling of peptides used for mass spectrometry-based assays, Clin. Chem. 62 (1) (2016) 48–69.

[8] Z. Patay, Metabolic disorders, in: P. Tortori-Donati, A. Rossi, R. Biancheri (Eds.), Pediatric Neuroradiology, Springer-Verlag, Berlin, 2005, pp. 543–722.

[9] H. Stibler, Direct immunofixation after isoelectric focusing, J. Neurol. Sci. 42 (1979) 275–281.

[10] E. Tham, E.A. Eklund, A. Hammarsjö, P. Bengtson, S. Geiberger, K. Lagerstedt-Robinson, H. Malmgren, D. Nilsson, G. Grigelionis, P. Conner, P. Lindgren, A. Lindstrand, A. Wedell, M. Albåge, K. Zielinska, A. Nordgren, N. Papadogiannakis, G. Nishimura, G. Grigelioniene, A novel phenotype in N-glycosylation disorders: Gillessen-Kaesbach-Nishimura skeletal dysplasia due to pathogenic variants in *ALG9*, Eur. J. Hum. Genet. 24 (2) (2015) 198–207.

[11] W. Vleugels, L. Keldermans, J. Jaeken, T.D. Butters, J.C. Michalski, G. Matthijs, F. Foulquier, Quality control of glycoproteins bearing truncated glycans in an ALG9-defective (CDG-IL) patient, Glycobiology 19 (2009) 910–917.

[12] M. Weinstein, E. Schollen, G. Matthijs, C. Neupert, T. Hennet, C.E. Grubenmann, C.G. Frank, M. Aebi, J.T.R. Clarke, A. Griffiths, L. Seargeant, N. Poplawski, CDG-IL: an infant with a novel mutation in the *ALG9* gene and additional phenotypic features, Am. J. Med. Genet. 136A (2005) 194–197.

[13] B. Xia, W. Zhang, X. Li, R. Jiang, T. Harper, R. Liu, R. Cummings, M. He, Serum N-glycan and O-glycan analysis by mass spectrometry for diagnosis of congenital disorders of glycosylation, Anal. Biochem. 442 (2) (2013) 178–185.